Tafoni formation at Theologos (Fthiotida, Greece)

Z. MODIANAKI[a], N. EVELPIDOU[a*], L. STAMATOPOULOS[b], M. STAMATAKIS[a]

Abstract. The aim of this paper is to provide further information of the tafoni development. At Theologos area, Fthiotis Prefecture, north Euboean Gulf, a carbonate formation hosts a variety of well developed tafoni. 165 tafoni were, randomly, selected by means of a detailed geomorphological investigation. The presence or absence of lichen cover, rock flaking, and cavern floor debris, amalgamation, salt flakes, different kind of structures, biological communities, were noted, while measurements regarding their dimension took place. Surface hardness values, obtained using a Schmidt hammer.

Although, there is no evidence of the key factor that drives the growth of tafoni, salt weathering and low strength seems determinant of their formation. Moreover, much of the evidences suggest that joints are actively influencing the origin and the morphology of tafoni. It is possible that tafoni formation is initiated at weak zones. The studied tafoni are actively developing and are not relict features inherited from a past environment. It seems that their evolutionary stage is II towards to III. The results of chemical and mineralogical analysis indicate that during the cavernous weathering, silica, sulphates, alumina and iron oxides have replaced carbonate grains. Also, at the non-weathered part of the rock, the main mineralogical phases are calcite and doplomite.

Keywords: Tafoni, flanking, cavernous weathering, carbonate weathering

Introduction

Tafoni are ellipsoidal, semi-cycle, natural rock openings both present in much different kind of rocks such as igneous and sedimentary rocks. Tafoni typically are developed by natural processes ant they, are divided into small openings, medium and larger cavern size. Tafoni are frequently characterized from complex cells like nests (Blackwelder, 1929; Smith, 1982; Pestrong, 1988; Hejl, 2005; Boxerman, 2006.

These cavernous weathering formations with various sizes and geometries are developed by different physical, chemical, biological and lithological conditions (Martini, 1978).

Tafoni are worldwide spread and common to coastal areas (Mellor et al., 1997), to moist areas (Goudie, 2003), to hot desert areas (Smith, 1978) and to cold desert areas (Calkin & Cailleux, 1962; Wellman & Wilson, 1965; Prebble, 1967; Matsouka, 1995; French & Guglielmin, 2000; Andre & Hall, 2004). Tafoni are rapidly developed in coastal environments, while in desert areas the procedure is slower. Tafoni are the 10% of coastal retreat reasons (Gill et al., 1981). Tafoni cause lots of damages to monuments, ports, coastal environments or damages to port protective constructions.

The study area, Theologos coastal zone, is located at the eastern part of Lokrida province, at the wider southeast part of Fthiotida Prefecture. Northeast side bordering North Euboean Gulf and South Atalanti Gulf is located (Fig. 1). The study area is far from human activities and some tafoni particularly those on the upper slopes of the study area, were inaccessible owing to slope steepness.

Theologos climate is classified into the mild areas of Greece with cool summers and mild winters. The mean annual temperature is 16.6°C and the mean annual rainfall height is 47.6 mm. Northwest wind is the dominant one affecting vitally the coast morphology during winter's months and east wind during summer (National Meteorological Service – Lamia Meteorological station). The main lithological formation of the studied area is comprised of Jurassic limestones (Maratos, 1965; Almpantakis, 1978).

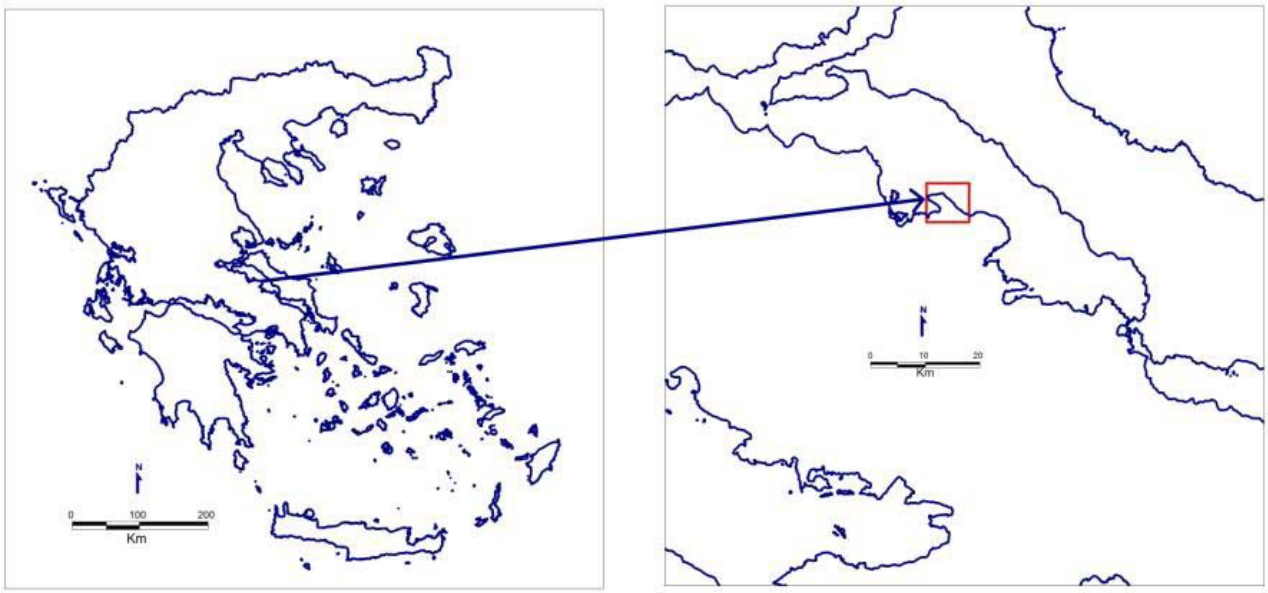

Figure 1. Location map of the studied area

Material and Methods

Fieldwork carried out during August and October 2011, included measurements in 165 tafoni (Table 1). Primary and secondly tafoni, were selected randomly. In order to gain some insight into local geological, topographic and hydrological controls on their formation, the area surrounding each measured tafoni was examined in terms of lithology, jointing, amalgamation and porosity (Table 2).

Each of the 165 tafoni was examined to provide details of its morphological characteristics. The morphological characteristics determined were (A) Width, of the opening parallel to the base, (B) Depth, which is the distance from the opening to the backwards of tafoni and (C) Height of the cavern floor and the direction of their opening (Fig. 2, Table 1).

For each measured tafone the exact location was recorded by GPS, as well as the occurrences of discontinuities cross or parallel to tafoni opening, visible salt efflorescence or concretions along the fractures internal or external tafoni, the existence of debris or epilithis lichens. Additionally, any visual disaggregation marks like flakes were recorded (Table 3).

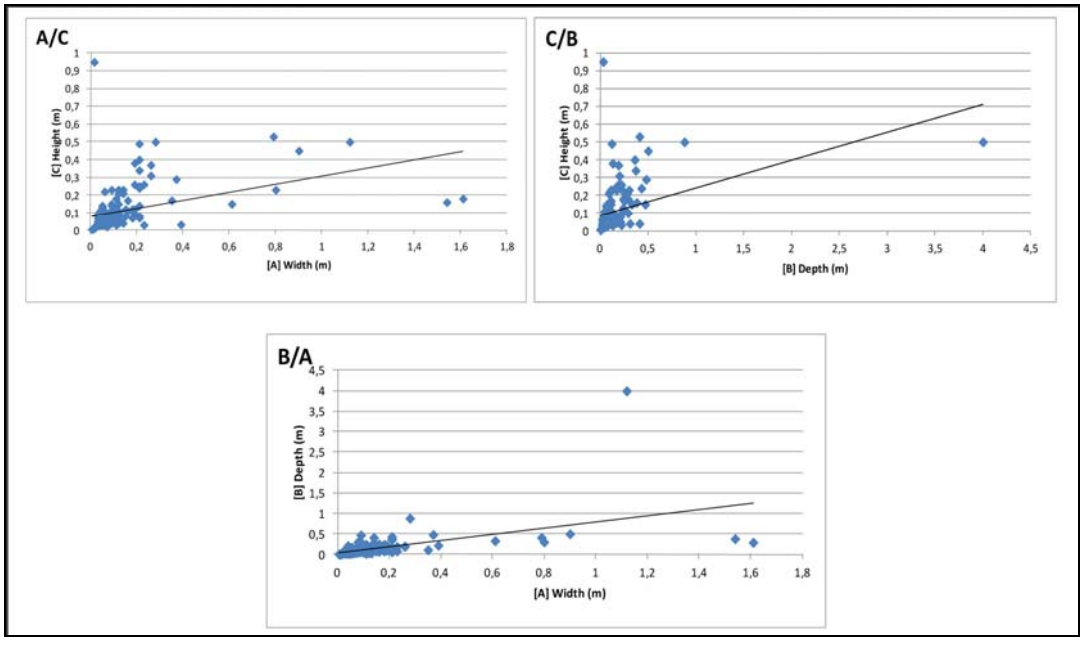

Figure 2. Cross plots of tafoni measurements: (a) width versus height, (b) depth versus height, (c) width versus depth

The surface hardness of each tafone was determined by a Schmidt hammer (low energy), a technique used in previous studies of cavernous weathering (Campbell, 1991). The measurements are taken from the smoothest surfaces of cavern visor, back wall, floor, ceiling, andouter roof, and also to non-weathered rock around the tafone (Table 4). In some cases, no values are taken due to technical problems. Firstly, the small size of the majority of studied tafoni is the main reason of the omitted values, as it prevented from the percussion. Moreover, some tafoni were standing without back or floor. Slick toolswere used when it wasneeded to normalize some rock surfaces.

The majority of the measurements are coming from backwall and floor of tafoni and almost in every casethere are measurements of the non-weathered rock. Two rebound values (R-values) were obtained from the same point at each site in order to ensure the accuracy of the measurements.

Four samples were collected from three tafoni (T2, T9, T110). Tafone 2 sample was picked from the backwall, while tafone 9 from the floor. From tafone 110 two samples were taken, one from the roof and one from the floor. Five thin sections were prepared and analyzed by the scanning electron microscope (SEM-ADS) JEOL JSM-5600 LINK ISIS combined with microanalyzer energy dispersive system OXFORD LINK ISIS 300, with software ZAF correction quantitative analysis at laboratories of the same university. The system was operating at 20 KV, 0.5 nA and 50 sec time of analysis. Both fresh and weathered surfaces were examined.

Results

Table 1 presents the morphological characteristics of the studied tafoni, the GPS location for each of them and also the samples origin. The dimensions of majority of the studied tafoni are smaller than 0.1 m. In fact, out of the 165 tafoni only 7 (T2: 0.9 m, T3: 0.8 m, T4: 1.54 m, T5: 1.61 m, T9: 1.12 m, T19: 0.79 m and T26: 0.61 m) have width ranging from 0.6 m up to 1.61 m (Fig. 3). The width of the 68.48% of the studied tafoni is smaller than 10 cm, while the dimensions of the smallest tafoni (T75) is 0.005 m. The depth of the 66.66% of the studied tafoni is smaller than 10 cm, while only two of them present extreme values i.e. T9 with depth of 4 m and T20 with a depth of 0.88 m (Fig. 4). Two tafoni presents high values in height; T19 with 0.53 m and T21 with 0.95 m, while 72,72% from the measured tafoni have height less than 10 cm (Fig. 5). The shape of most of the tafoni is characterized by the width being larger than depth (51.51% of the measurements), while in 56.36% of the measurements width is larger than height (Table 1). Also, the strongest correlation among the indicators is width versus depth.

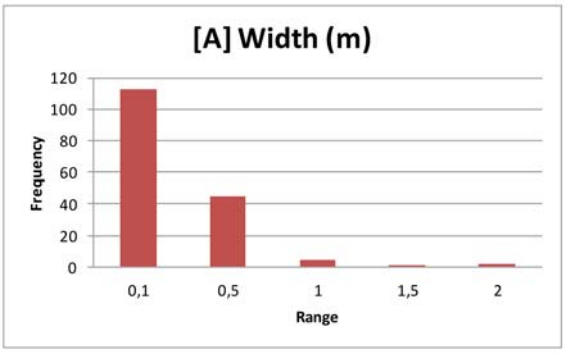

Figure 3. Histogram of width [A] dimension of the studied tafoni

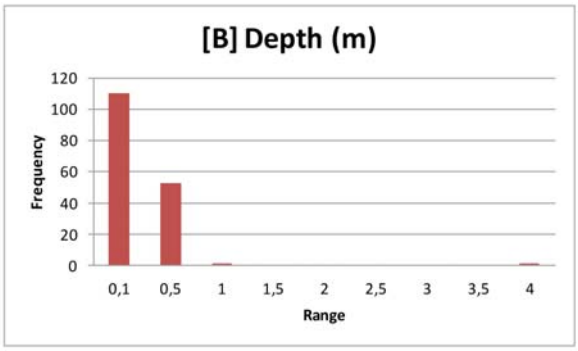

Figure 4. Histogram of depth [B] dimension of the studied tafoni

The mean height of the measured caverns is 0.1 m (Table 1), while the mean width and the mean depth are 0.13 m wide and 0.14 m deep. The largest cavern is 0.5 m high, 1.12 m wide, 4 m deep (T9) and the smallest with an accurate correlation among the indicators precisely at 0.005 m (T75).

Secondary caverns are recorded inside primaries separated by compartments and remnants of walls (Fig. 6). The 3.63% of the investigated tafoni present cavern visor with flaking playing the most important role in active rock weathering since it is occurring in 45.45% of the studied tafoni. Finally, the 22.42% of the studied tafoni presents debris inside the cavern (Fig. 7).

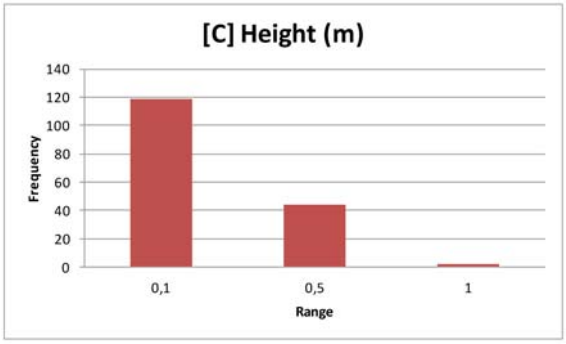

Figure 5. Histogram of height [C] dimension of the studied tafoni

Figure 6. Two separated tafoni are jointed in the backwall because of vertical wall destruction

Figure 7. Cavern floor debris

Table 4 presents the results from the tafoni percussions to the interior or the exterior as well as to the non-weathered tafoni surface. Based on these measurements, the difference between non-weathered rock surface and tafoni surface is less than 5 MPa. Measurements from non-weathered carbonates are ranging 10-20%, while only the 23.02% of measurements are lower than 20%. Rock hardness measurements indicate that R – values on the cavern visor and backwall are higher than those taken from the floor. In fact, 25% of measurements taken from the cavern visor are lower than 20%, while from the floor this percentage is getting lower (13.33%). The 75% of the measurements taken from the ceiling and the outer surface of the tafoni are ranging from 10 to 20%.

Lichens cover the outer surface only of 4 tafoni (T21, T128, T149, T159).

The 5 thin sections examined by the SEM-EDS system, showed that the majority of fresh rock surfaces are composed by calcite and dolomite. The weathered surfaces often contain silica, sulphates, alumina and iron-oxides and phosphates in minor amounts low rates (Fig. 8-10). The origin of these imurities is much likely originated from the erosion of the surrounding rocks and also the sea water [sulphates]. As it is revelated by the SEM images and analysis of each component, these phases have replaced calcite and dolomite crystals, grain by grain [peudomorphosis].

Figure 8. SEM microphotograph of tafoni's 2 thin section [fresh side] (50% CaO, 0.45% MgO, 0.08% FeO)

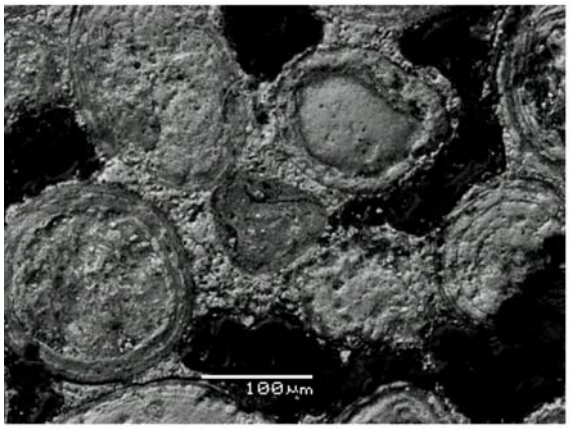

Figure 9. SEM microphotograph of tafoni's 2 thin section [weathered side] (39.45% CaO, 1.67% MgO, 3.18% SiO_2, 0.68% Al_2O_3, 0.66% SO_4)

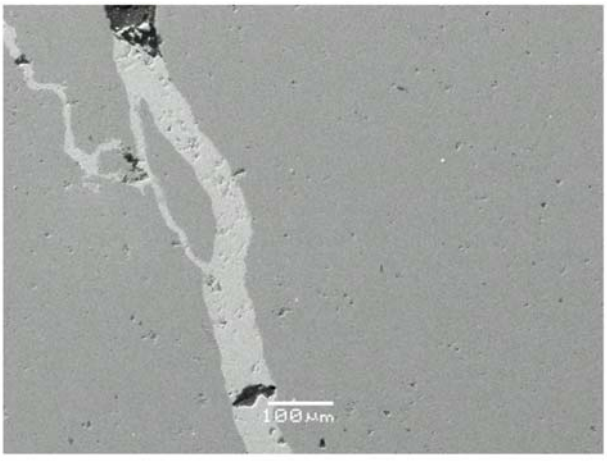

Figure 10. SEM microphotograph of tafoni's 2 thin section [fresh side] (29.12% CaO, 19.57% MgO)

Discussion-Conclusions

Theologos tafoni are both primary and embedded, developed because of joints. Salt weathering has played a significant role; silica, sulphates and alumina have replaced calcite and dolomite. The floor of many studied caverns was covered by debris indicating the active evolutionary stage. The fresh rock is almost exclusively composed of dolomite and calcite.

The morphology of tafoni evidences that the evolutionary stage according to Boxerman (2006) in II because most of the tafoni grow more in depth direction than parallel to the opening. In some locations, though, we believe that the evolutionary stage is II to III especially to the west side of the coast, because of the collapse of intermediate walls and further cavern enlargement.

Schmidt hammer measurements present a harder cavern visor and backwall instead of floor, ceiling or outer surface. Cavern visor results are consistent to coastal tafoni generally, but backwall results come in conflict to previous studies (Mottershead and Pye, 1994).

Substantially, tafoni development and enlargement is not only a salt weathering phenomenon but it is also relating with weak surfaces, joints and fractures.

Acknowledgements

Niki Evelpidou would like to thank Victor Sabot for the inspiration of this kind of research.

Authors would like to thank EDAFOMIXANIKI Ltd for their kindness to provide the Schmidt Hammer equipment. Finally, authors would like to thank Anastasios Modianakis, Olga Zorba, Aristotelis Kartanos, Yiannis Sfiris, Maria Mouzakiti and Christos Geramoutsos for their contribution during fieldwork and to Eleana Karkani for her contribution to laboratory work.

REFERENCES

Almpantakis, I.G.M.S. 1970. Geological map of Greece, sheet Larymna 1:50.000.

Andre, M.-F., Hall, K., 2004. Honeycomb development on Alexander Island, glacial history of George VI Sound and palaeoclimatic implications (Two Step Cliffs/Mars Oasis, W. Antarctica): Geomorphology, v. 65, p. 117-138. BC: Geomorphology, v. 64, p. 87-95.

Blackwelder, E., 1929. Cavernous Rock Surfaces of the Desert: American Journal of Science, v. 17, p. 393-99.

Boxerman J., 2006. The Evolution of Tafoni on Coastal Sandstones in Northern California, Unpublished Master's Thesis, Department of Geoscience, San Francisco State University, May, 2006.

Calkin, P., Cailleux, A., 1962. A Quantitative Study of Cavernous Weathering (Taffonis) and its Application to Glacial Chronology in Victoria Valley, Antarctica: Zeitschrift fuer Geomorphologie, v. 6, p. 317-324.

Campbell, I.A., 1991. Classification of rock weathering at Writing-On-Stone Provincial Park Alberta, CanadaQ a study in applied geomorphology, Earth Surface Processes and Landforms, 16: 70-711.

French, H.M., Guglielmin, M., 2000. Cryogenic weathering of granite, Northern Victoria Land, Antarctica: Permafrost and Periglacial Processes, v. 11, p. 305-314.

Gill, E.D., Segnit, E.R., McNeill, N.H., 1981. Rate of Formation of Honeycomb Weathering Features (Small Scale Tafoni) on the Otway Coast, S.E. Australia: Preceedings of the Royal Society of Victoria, v. 92, p. 149-154.

Goudie A., 2003. Encyclopedia of geomorphology, London, Routledge, p. 1200.

Hejl, E., 2005. A Pictorial Study of Tafoni Development from the 2nd Millennium.

I.G.M.S. 1965, 1970. Geological maps 1:50.000 maps: Atalanti, Larimna.

Maratos I.G.M.S., 1965. Atalantis geological map 1:50.000.

Martini, I.P., 1978. Tafoni Weathering, with Examples from Tuscany, Italy: Zeitschrift fuer Geomorphologie, v. 22, p. 44-67.

Matsouka, N., 1995. Rock weathering processes and landform development in the Sor Rondane Mountains, Antarctica: Geomophology, v. 12, p. 323-329.

Mellor, A., Short, J., Kirkby, S.J., 1997. Tafoni in the El Chorro Area, Andalucia, Southern Spain: Earth Surfaces Processes and Landforms, v. 22, p. 817-833.

Mottershead, D.N., Pye, K., 1994. Tafoni on coastal slopes, South Devon, U.K.: Earth surfaces processes and Landforms, v. 19, p. 543-563.

National Meteorological Service – Lamia Meteorological station.

Pestrong, R., 1988. Tafoni Weathering of Old Structures Along the Northern California Coast, USA: Proceedings of an International Symposium Organized by the Greek National Group of IAEG, p. 1049-105.

Prebble, M.M., 1967. Cavernous Weathering in the Taylor Dry Valley, Victoria Land, Antarctica: Nature, v. 216, p. 1194-1195.

Smith, P.J., 1982. Why Honeycomb Weathering: Nature, v. 298, p. 121-122.

Smith, P.J., 1978. The origin and geomorphic implications of Cliff foot recesses and tafoni on limestone Hamadas in the Northwest Sahara: Zeitschrift fuer Geomorphologie, v. 22, p. 21-43.

Wellman, H.W., Wilson, A.T., 1965. Salt Weathering, a Neglected Geological Erosive Agent in Coastal and Arid Environments: Nature, v. 205, p. 1097-1098.

Table 1. Main morphological characteristics of the studied tafoni

Tafoni	y coords	x coords	A] Width. (m)	[B] Depth. (m)	[C] Height. (m)	[A]-[B]	[A]-[C]	[A]/[B]	[C]/[B]
T1	38° 40.440N	23° 10.206E	0.26	0.2	0.31	0.06	-0.05	1.3	1.55
T2	38° 40.445N	23° 10.202E	0.9	0.5	0.45	0.4	0.45	1.8	0.9
T3	38° 40.443N	23° 10.203E	0.8	0.3	0.23	0.5	0.57	2.66	0.76
T4	38° 40.447N	23° 10.194E	1.54	0.39	0.14	1.15	1.4	4.05	0.42
T5	38° 40.441N	23° 10.196E	1.61	0.33	0.26	1.28	1.35	5.55	0.62
T6	38° 40.444N	23° 10.196E	0.37	0.48	0.29	-0.11	0.08	0.77	0.6
T7	38° 40.448N	23° 10.196E	0.35	0.2	0.17	0.15	0.18	3.18	1.54
T8	38° 40.446N	23° 10.191E	0.21	0.36	0.4	-0.15	-0.19	0.58	1.11
T9	38° 40.445N	23° 10.190E	1.12	4	0.5	-2.88	0.62	0.28	0.12
T10	38° 40.447N	23° 10.189E	0.12	0.09	0.21	0.03	-0.09	1.33	2.33
T11	38° 40.447N	23° 10.187E	0.19	0.21	0.09	-0.02	0.1	0.9	0.42
T12	38° 40.428N	23° 10.183E	0.08	0.21	0.09	-0.13	-0.01	0.38	0.42
T13	38° 40.446N	23° 10.180E	0.21	0.43	0.24	-0.22	-0.03	0.48	0.55
T14	38° 40.439N	23° 10.178E	0.22	0.37	0.34	-0.15	-0.12	0.56	0.91
T15	38° 40.440N	23° 10.177E	0.14	0.23	0.23	-0.09	-0.09	0.6	1
T16	38° 40.439N	23° 10.173E	0.04	0.05	0.05	-0.01	-0.01	0.8	1
T17	38° 40.436N	23° 10.163E	0.06	0.11	0.05	-0.05	0.01	0.54	0.45
T18	38° 40.435N	23° 10.161E	0.1	0.1	0.09	0	0.01	1	0.9
T19	38° 40.436N	23° 10.159E	0.79	0.41	0.53	0.38	0.26	1.92	1.29
T20	38° 40.436N	23° 10.157E	0.28	0.88	0.5	-0.6	-0.22	0.31	0.56
T21	38° 40.436N	23° 10.155E	0.015	0.03	0.95	-0.015	-0.935	0.5	31.67
T22	38° 40.434N	23° 10.154E	0.19	0.13	0.38	0.06	-0.19	1.46	2.92
T23	38° 40.435N	23° 10.153E	0.08	0.17	0.08	-0.09	0	0.47	0.47
T24	38° 40.434N	23° 10.148E	0.09	0.07	0.08	0.02	0.01	1.28	1.14
T25	38° 40.434N	23° 10.147E	0.05	0.06	0.05	-0.01	0	0.83	0.83
T26	38° 40.430N	23° 10.135E	0.61	0.33	0.15	0.28	0.46	1.84	0.45
T27	38° 40.430N	23° 10.132E	0.015	0.005	0.01	0.01	0.005	3	2
T28	38° 40.432N	23° 10.130E	0.15	0.09	0.12	0.06	0.03	1.66	1.33
T29	38° 40.431N	23° 10.136E	0.025	0.03	0.03	-0.005	-0.005	0.83	1
T30	38° 40.433N	23° 10.139E	0.04	0.07	0.03	-0.03	0.01	0.57	0.42
T31	38° 40.433N	23° 10.139E	0.07	0.04	0.02	0.03	0.05	1.75	0.5
T32	38° 40.434N	23° 10.143E	0.08	0.07	0.05	0.01	0.03	1.14	0.71
T33(9A)	38° 40.445N	23° 10.190E	0.21	0.12	0.49	0.09	-0.28	1.75	4.08
T34(9B)	38° 40.445N	23° 10.190E	0.16	0.25	0.17	-0.09	-0.01	0.64	0.68
T35(9Γ)	38° 40.445N	23° 10.190E	0.16	0.07	0.11	0.09	0.05	2.28	1.57
T36(9Δ)	38° 40.445N	23° 10.190E	0.05	0.07	0.14	-0.02	-0.09	0.71	2
T37	38° 40.449N	23° 10.193E	0.26	0.19	0.37	0.07	-0.11	1.36	1.94
T38	38° 40.449N	23° 10.192E	0.06	0.1	0.22	-0.04	-0.16	0.6	2.2
T39	38° 40.449N	23° 10.192E	0.06	0.06	0.07	0	-0.01	1	1.16
T40	38° 40.449N	23° 10.192E	0.04	0.06	0.11	-0.02	-0.07	0.66	1.83
T41(7A)	38° 40.448N	23° 10.196E	0.14	0.28	0.21	-0.14	-0.07	0.5	0.75
T42(7B)	38° 40.448N	23° 10.196E	0.09	0.1	0.08	-0.01	0.01	0.9	0.8
T43(7Γ)	38° 40.448N	23° 10.196E	0.04	0.07	0.05	-0.03	-0.01	0.57	0.71

T44(7Δ)	38° 40.448N	23° 10.196E	0.03	0.03	0.04	0	-0.01	1	1.33
T45	38° 40.448N	23° 10.196E	0.05	0.07	0.04	-0.02	0.01	0.71	0.57
T46	38° 40.448N	23° 10.196E	0.06	0.12	0.09	-0.06	-0.03	0.5	0.75
T47	38° 40.447N	23° 10.195E	0.08	0.05	0.09	0.03	-0.01	1.6	1.8
T48	38° 40.448N	23° 10.195E	0.15	0.08	0.08	0.07	0.07	1.875	1
T49(48A)	38° 40.448N	23° 10.195E	0.04	0.16	0.06	-0.12	-0.02	0.25	0.37
T50	38° 40.448N	23° 10.195E	0.14	0.41	0.04	-0.27	0.1	0.34	0.09
T51	38° 40.447N	23° 10.203E	0.1	0.12	0.06	-0.02	0.04	0.83	0.5
T52	38° 40.447N	23° 10.203E	0.04	0.07	0.04	-0.03	0	0.57	0.57
T53	38° 40.447N	23° 10.201E	0.09	0.29	0.1	-0.2	-0.01	0.31	0.34
T54	38° 40.441N	23° 10.195E	0.1	0.14	0.06	-0.04	0.04	0.71	0.42
T55	38° 40.447N	23° 10.199E	0.23	0.19	0.26	0.04	-0.03	1.21	1.36
T56(2A)	38° 40.445N	23° 10.202E	0.18	0.11	0.07	0.07	0.11	1.63	0.63
T57	38° 40.446N	23° 10.202E	0.05	0.02	0.06	0.03	-0.01	2.5	3
T58	38° 40.446N	23° 10.202E	0.09	0.07	0.08	0.02	0.01	1.28	1.14
T59	38° 40.446N	23° 10.202E	0.05	0.06	0.08	-0.01	-0.03	0.83	1.33
T60	38° 40.446N	23° 10.202E	0.03	0.05	0.09	-0.02	-0.06	0.6	1.8
T61(5A)	38° 40.441N	23° 10.196E	0.08	0.29	0.1	-0.21	-0.02	0.27	0.34
T62(5B)	38° 40.441N	23° 10.196E	0.11	0.24	0.18	-0.13	-0.07	0.45	0.75
T63	38° 40.444N	23° 10.205E	0.06	0.1	0.04	-0.04	0.02	0.6	0.4
T64(63A)	38° 40.445N	23° 10.203E	0.055	0.06	0.03	-0.005	0.025	0.91	0.5
T65	38° 40.445N	23° 10.201E	0.21	0.06	0.08	0.15	0.13	3.5	1.33
T66(65A)	38° 40.445N	23° 10.201E	0.07	0.11	0.06	-0.04	0.01	0.63	0.54
T67(65B)	38° 40.445N	23° 10.201E	0.04	0.03	0.04	0.01	0	1.33	1.33
T68	38° 40.448N	23° 10.207E	0.1	0.24	0.13	-0.14	-0.03	0.41	0.54
T69	38° 40.448N	23° 10.207E	0.03	0.04	0.03	-0.01	0	0.75	0.75
T70	38° 40.448N	23° 10.207E	0.035	0.06	0.04	-0.025	-0.005	0.58	0.66
T71	38° 40.440N	23° 10.204E	0.09	0.07	0.04	0.02	0.05	1.28	0.57
T72	38° 40.440N	23° 10.204E	0.06	0.07	0.05	-0.01	0.01	0.85	0.71
T73	38° 40.445N	23° 10.206E	0.1	0.09	0.08	0.01	0.02	1.11	0.88
T74	38° 40.444N	23° 10.205E	0.19	0.22	0.26	-0.03	-0.07	0.86	1.18
T75	38° 40.444N	23° 10.205E	0.005	0.005	0.005	0	0	1	1
T76	38° 40.445N	23° 10.205E	0.05	0.05	0.07	0	-0.02	1	1.4
T77	38° 40.445N	23° 10.205E	0.03	0.13	0.03	-0.1	0	0.23	0.23
T78	38° 40.443N	23° 10.206E	0.23	0.08	0.03	0.15	0.2	2.87	0.37
T79	38° 40.444N	23° 10.206E	0.04	0.08	0.07	-0.04	-0.03	0.5	0.87
T80	38° 40.449N	23° 10.302E	0.12	0.04	0.04	0.08	0.08	3	1
T81(80A)	38° 40.449N	23° 10.302E	0.03	0.05	0.03	-0.02	0	0.6	0.6
T82(80B)	38° 40.449N	23° 10.302E	0.03	0.03	0.03	0	0	1	1
T83(80Γ)	38° 40.449N	23° 10.302E	0.01	0.005	0.01	0.005	0	2	2
T84	38° 40.444N	23° 10.206E	0.06	0.08	0.11	-0.02	-0.05	0.75	1.375
T85	38° 40.444N	23° 10.206E	0.07	0.05	0.06	0.02	0.01	1.4	1.2
T86	38° 40.448N	23° 10.203E	0.04	0.04	0.04	0	0	1	1
T87	38° 40.448N	23° 10.203E	0.03	0.05	0.05	-0.02	-0.02	0.6	1
T88	38° 40.431N	23° 10.213E	0.21	0.15	0.07	0.06	0.14	1.4	0.46

T89	38° 40.431N	23° 10.213E	0.08	0.06	0.06	0.02	0.02	1.33	1
T90	38° 40.429N	23° 10.215E	0.19	0.1	0.12	0.09	0.07	1.9	1.2
T91(90A)	38° 40.429N	23° 10.215E	0.12	0.06	0.09	0.06	0.03	2	1.5
T92(90B)	38° 40.429N	23° 10.215E	0.11	0.1	0.08	0.01	0.03	1.1	0.8
T93	38° 40.446N	23° 10.208E	0.05	0.16	0.06	-0.11	-0.01	0.31	0.37
T94	38° 40.448N	23° 10.207E	0.21	0.17	0.25	0.04	-0.04	1.23	1.47
T95(94A)	38° 40.448N	23° 10.206E	0.05	0.04	0.045	0.01	0.005	1.25	1.12
T96	38° 40.451N	23° 10.206E	0.05	0.045	0.09	0.005	-0.04	1.11	2
T97	38° 40.450N	23° 10.206E	0.03	0.05	0.07	-0.02	-0.04	0.6	1.4
T98	38° 40.450N	23° 10.206E	0.045	0.04	0.03	0.005	0.015	1.12	0.75
T99(98A)	38° 40.450N	23° 10.206E	0.02	0.04	0.025	-0.02	-0.005	0.5	0.62
T100(98B)	38° 40.450N	23° 10.206E	0.035	0.035	0.03	0	0.005	1	0.85
T101	38° 40.446N	23° 10.207E	0.08	0.08	0.045	0	0.035	1	0.56
T102	38° 40.452N	23° 10.206E	0.11	0.06	0.03	0.05	0.08	1.83	0.5
T103(102A)	38° 40.452N	23° 10.206E	0.06	0.05	0.035	0.01	0.025	1.2	0.7
T104(102B)	38° 40.452N	23° 10.206E	0.055	0.17	0.045	-0.115	0.01	0.32	0.26
T105	38° 40.446N	23° 10.206E	0.045	0.05	0.05	-0.005	-0.005	0.9	1
T106	38° 40.446N	23° 10.206E	0.04	0.08	0.065	-0.04	-0.025	0.5	0.8125
T107	38° 40.437N	23° 10.207E	0.09	0.11	0.15	-0.02	-0.06	0.81	1.36
T108	38° 40.451N	23° 10.203E	0.09	0.09	0.1	0	-0.01	1	1.11
T109(108A)	38° 40.451N	23° 10.203E	0.04	0.1	0.07	-0.06	-0.03	0.4	0.7
T110	38° 40.448N	23° 10.205E	0.39	0.22	0.032	0.17	0.358	1.77	0.14
T111	38° 40.451N	23° 10.200E	0.05	0.08	0.13	-0.03	-0.08	0.62	1.62
T112	38° 40.452N	23° 10.201E	0.04	0.08	0.05	-0.04	-0.01	0.5	0.62
T113	38° 40.446N	23° 10.187E	0.18	0.08	0.11	0.1	0.07	2.25	1.37
T114	38° 40.446N	23° 10.186E	0.05	0.04	0.05	0.01	0	1.25	1.25
T115	38° 40.447N	23° 10.186E	0.06	0.03	0.05	0.03	0.01	2	1.66
T116	38° 40.444N	23° 10.181E	0.07	0.06	0.09	0.01	-0.02	1.16	1.5
T117	38° 40.447N	23° 10.183E	0.045	0.045	0.11	0	-0.065	1	2.44
T118	38° 40.447N	23° 10.183E	0.06	0.11	0.075	-0.05	-0.015	0.54	0.68
T119	38° 40.447N	23° 10.183E	0.035	0.05	0.04	-0.015	-0.005	0.7	0.8
T120	38° 40.446N	23° 10.183E	0.045	0.055	0.03	-0.01	0.015	0.81	0.54
T121	38° 40.448N	23° 10.183E	0.12	0.045	0.07	0.075	0.05	2.66	1.55
T122	38° 40.446N	23° 10.183E	0.045	0.05	0.04	-0.005	0.005	0.9	0.8
T123	38° 40.447N	23° 10.184E	0.04	0.1	0.05	-0.06	-0.01	0.4	0.5
T124	38° 40.446N	23° 10.184E	0.04	0.025	0.07	0.015	-0.03	1.6	2.8
T125	38° 40.440N	23° 10.177E	0.045	0.04	0.035	0.005	0.01	1.125	0.87
T126	38° 40.441N	23° 10.176E	0.12	0.11	0.23	0.01	-0.11	1.09	2.09
T127	38° 40.440N	23° 10.177E	0.12	0.07	0.15	0.05	-0.03	1.71	2.14
T128	38° 40.440N	23° 10.177E	0.04	0.1	0.04	-0.06	0	0.4	0.4
T129	38° 40.438N	23° 10.169E	0.05	0.11	0.08	-0.06	-0.03	0.45	0.72
T130	38° 40.438N	23° 10.168E	0.035	0.035	0.04	0	-0.005	1	1.14
T131	38° 40.434N	23° 10.163E	0.065	0.06	0.05	0.005	0.015	1.08	0.83
T132	38° 40.436N	23° 10.162E	0.05	0.06	0.04	-0.01	0.01	0.83	0.66
T133	38° 40.436N	23° 10.162E	0.09	0.17	0.23	-0.08	-0.14	0.52	1.35

T134(19A)	38° 40.436N	23° 10.159E	0.21	0.09	0.14	0.12	0.07	2.33	1.55
T135(19B)	38° 40.436N	23° 10.159E	0.1	0.05	0.1	0.05	0	2	2
T136(19Γ)	38° 40.436N	23° 10.159E	0.07	0.05	0.04	0.02	0.03	1.4	0.8
T137(19Δ)	38° 40.436N	23° 10.159E	0.13	0.03	0.07	0.1	0.06	4.33	2.33
T138	38° 40.436N	23° 10.159E	0.09	0.06	0.14	0.03	-0.05	1.5	2.33
T139(138A)	38° 40.436N	23° 10.159E	0.08	0.31	0.04	-0.23	0.04	0.25	0.12
T140(138B)	38° 40.436N	23° 10.159E	0.04	0.21	0.05	-0.17	-0.01	0.19	0.23
T141	38° 40.438N	23° 10.160E	0.13	0.08	0.08	0.05	0.05	1.62	1
T142(141A)	38° 40.438N	23° 10.160E	0.04	0.04	0.06	0	-0.02	1	1.5
T143	38° 40.438N	23° 10.159E	0.05	0.08	0.05	-0.03	0	0.62	0.62
T144	38° 40.442N	23° 10.161E	0.035	0.02	0.03	0.015	0.005	1.75	1.5
T145	38° 40.437N	23° 10.161E	0.045	0.03	0.045	0.015	0	1.5	1.5
T146	38° 40.437N	23° 10.161E	0.08	0.1	0.09	-0.02	-0.01	0.8	0.9
T147	38° 40.437N	23° 10.161E	0.09	0.47	0.15	-0.38	-0.06	0.19	0.31
T148	38° 40.439N	23° 10.160E	0.08	0.11	0.08	-0.03	0	0.72	0.72
T149	38° 40.441N	23° 10.160E	0.05	0.04	0.035	0.01	0.015	1.25	0.87
T150	38° 40.439N	23° 10.156E	0.18	0.24	0.12	-0.06	0.06	0.75	0.5
T151(150A)	38° 40.439N	23° 10.156E	0.11	0.21	0.08	-0.1	0.03	0.52	0.38
T152(150B)	38° 40.439N	23° 10.156E	0.11	0.02	0.04	0.09	0.07	5.5	2
T153(150Γ)	38° 40.439N	23° 10.156E	0.05	0.09	0.04	-0.04	0.01	0.55	0.44
T154	38° 40.436N	23° 10.160E	0.07	0.04	0.07	0.03	0	1.75	1.75
T155(154A)	38° 40.436N	23° 10.160E	0.045	0.04	0.045	0.005	0	1.125	1.12
T156(154B)	38° 40.436N	23° 10.160E	0.03	0.03	0.025	0	0.005	1	0.83
T157	38° 40.436N	23° 10.159E	0.07	0.06	0.09	0.01	-0.02	1.16	1.5
T158	38° 40.439N	23° 10.160E	0.04	0.045	0.04	-0.005	0	0.88	0.88
T159	38° 40.434N	23° 10.160E	0.07	0.07	0.09	0	-0.02	1	1.28
T160	38° 40.434N	23° 10.159E	0.12	0.1	0.11	0.02	0.01	1.2	1.1
T161	38° 40.435N	23° 10.159E	0.05	0.07	0.06	-0.02	-0.01	0.71	0.85
T162	38° 40.436N	23° 10.159E	0.05	0.06	0.05	-0.01	0	0.83	0.83
T163	38° 40.433N	23° 10.142E	0.12	0.07	0.1	0.05	0.02	1.71	1.42
T164	38° 40.447N	23° 10.151E	0.05	0.13	0.1	-0.08	-0.05	0.38	0.76
T165	38° 40.447N	23° 10.151E	0.06	0.11	0.08	-0.05	-0.02	0.54	0.72

Table 2. Recorded joints, amalgamation, and porosity for each tafoni

Tafoni	Parallel Joints (Yes/No)	Cross Joints (Yes/No)	Amalgamation (Yes/No)	Porosity (Yes/No)
T1	No	No	Yes	No
T2	Yes	Yes	Yes	Yes
T3	Yes	Yes	Yes	Yes
T4	Yes	Yes	Yes	Yes
T5	Yes	Yes	Yes	Yes
T6	Yes	Yes	Yes	Yes
T7	No	No	Yes	Yes
T8	Yes	No	Yes	Yes
T9	Yes	Yes	Yes	Yes
T10	No	No	Yes	Yes
T11	Yes	No	Yes	Yes
T12	No	No	Yes	No
T13	Yes	Yes	Yes	No
T14	Yes	No	Yes	No
T15	No	No	Yes	Yes
T16	No	No	Yes	No
T17	Yes	No	Yes	Yes
T18	No	No	Yes	No
T19	Yes	Yes	Yes	Yes
T20	Yes	Yes	Yes	Yes
T21	No	No	Yes	No
T22	No	No	Yes	Yes
T23	No	No	Yes	Yes
T24	No	No	Yes	No
T25	No	No	Yes	No
T26	Yes	Yes	Yes	Yes
T27	No	No	Yes	No
T28	No	No	Yes	No
T29	Yes	No	Yes	Yes
T30	No	No	Yes	No
T31	No	No	Yes	Yes
T32	No	No	Yes	Yes
T33(9A)	Yes	Yes	Yes	Yes
T34(9B)	Yes	Yes	Yes	No
T35(9Γ)	Yes	Yes	Yes	Yes
T36(9Δ)	Yes	Yes	Yes	Yes
T37	Yes	Yes	Yes	Yes
T38	No	No	Yes	No
T39	No	No	Yes	No
T40	Yes	Yes	Yes	Yes
T41(7A)	No	No	Yes	Yes
T42(7B)	No	No	Yes	Yes
T43(7Γ)	No	No	Yes	No
T44(7Δ)	No	No	Yes	No
T45	No	No	Yes	No
T46	No	No	Yes	No
T47	No	No	Yes	Yes
T48	No	No	Yes	No
T49(48A)	No	No	Yes	No
T50	No	No	Yes	Yes
T51	Yes	No	Yes	Yes
T52	Yes	No	Yes	Yes
T53	Yes	Yes	Yes	Yes
T54	No	No	Yes	Yes
T55	Yes	Yes	Yes	Yes
T56(2A)	Yes	Yes	Yes	Yes
T57	Yes	No	Yes	No
T58	No	No	Yes	No
T59	No	No	Yes	Yes
T60	No	No	Yes	Yes
T61(5A)	Yes	No	Yes	Yes
T62(5B)	Yes	No	Yes	Yes
T63	No	No	Yes	No
T64(63A)	No	No	Yes	No
T65	Yes	Yes	Yes	Yes
T66(65A)	Yes	Yes	Yes	Yes
T67(65B)	Yes	Yes	Yes	Yes
T68	No	No	Yes	No
T69	No	No	Yes	No
T70	No	No	Yes	No
T71	No	No	Yes	No
T72	No	No	Yes	No
T73	No	Yes	Yes	Yes
T74	No	No	Yes	Yes
T75	No	No	Yes	No
T76	No	Yes	Yes	Yes
T77	No	Yes	Yes	Yes
T78	No	No	Yes	No
T79	Yes	Yes	Yes	Yes
T80	No	No	Yes	Yes
T81(80A)	No	No	Yes	Yes

T82(80B)	No	No	Yes	Yes
T83(80Γ)	No	No	Yes	No
T84	No	Yes	Yes	Yes
T85	No	Yes	Yes	Yes
T86	Yes	No	Yes	Yes
T87	Yes	No	Yes	Yes
T88	Yes	Yes	Yes	Yes
T89	Yes	Yes	Yes	No
T90	No	Yes	Yes	No
T91(90A)	No	Yes	Yes	No
T92(90B)	No	Yes	Yes	No
T93	Yes	Yes	Yes	No
T94	Yes	Yes	Yes	Yes
T95(94A)	Yes	Yes	Yes	Yes
T96	No	No	Yes	No
T97	No	No	Yes	No
T98	Yes	No	Yes	Yes
T99(98A)	Yes	No	Yes	Yes
T100(98B)	Yes	No	Yes	Yes
T101	Yes	No	Yes	No
T102	Yes	No	Yes	Yes
T103(102A)	Yes	No	Yes	Yes
T104(102B)	Yes	No	Yes	Yes
T105	No	No	Yes	No
T106	No	No	Yes	Yes
T107	No	No	Yes	Yes
T108	Yes	No	Yes	Yes
T109(108A)	Yes	No	Yes	No
T110	Yes	Yes	Yes	Yes
T111	Yes	Yes	Yes	Yes
T112	Yes	Yes	Yes	Yes
T113	Yes	Yes	Yes	Yes
T114	Yes	Yes	Yes	Yes
T115	No	No	Yes	Yes
T116	No	No	Yes	No
T117	No	No	Yes	Yes
T118	No	No	Yes	Yes
T119	No	No	Yes	Yes
T120	No	No	Yes	Yes
T121	No	No	Yes	No
T122	No	No	Yes	No

T123	No	No	Yes	No
T124	No	No	Yes	Yes
T125	No	No	Yes	Yes
T126	No	No	Yes	Yes
T127	No	No	Yes	Yes
T128	Yes	Yes	Yes	No
T129	No	No	Yes	Yes
T130	No	No	Yes	Yes
T131	Yes	Yes	Yes	Yes
T132	No	No	Yes	No
T133	Yes	Yes	Yes	No
T134(19A)	Yes	Yes	Yes	Yes
T135(19B)	Yes	Yes	Yes	Yes
T136(19Γ)	Yes	Yes	Yes	No
T137(19Δ)	Yes	Yes	Yes	Yes
T138	Yes	Yes	Yes	Yes
T139(138A)	Yes	Yes	Yes	Yes
T140(138B)	Yes	Yes	Yes	Yes
T141	No	No	Yes	Yes
T142(141A)	No	No	Yes	Yes
T143	No	No	Yes	Yes
T144	No	No	Yes	Yes
T145	No	Yes	Yes	No
T146	No	Yes	Yes	Yes
T147	No	Yes	Yes	Yes
T148	Yes	No	Yes	Yes
T149	No	No	Yes	Yes
T150	Yes	Yes	Yes	Yes
T151(150A)	Yes	Yes	Yes	Yes
T152(150B)	Yes	Yes	Yes	Yes
T153(150Γ)	Yes	Yes	Yes	Yes
T154	Yes	Yes	Yes	Yes
T155(154A)	Yes	Yes	Yes	Yes
T156(154B)	Yes	Yes	Yes	Yes
T157	Yes	Yes	Yes	Yes
T158	Yes	Yes	Yes	Yes
T159	No	No	Yes	Yes
T160	No	No	Yes	Yes
T161	No	No	Yes	Yes
T162	No	No	Yes	Yes
T163	Yes	Yes	Yes	Yes
T164	Yes	Yes	Yes	Yes
T165	Yes	Yes	Yes	Yes

Table 3. Other surface elements

Tafoni	Cavern visor	Flakes	Lichens	Debris	Salt
T1		■			
T2	■	■		■	
T3		■		■	
T4		■			
T5					
T6		■		■	
T7		■		■	■
T8		■			
T9		■		■	
T10					
T11	■				
T12		■			
T13		■		■	
T14		■			
T15		■			
T16				■	
T17					
T18				■	
T19		■			■
T20		■			■
T21			■		
T22		■			■
T23		■			■
T24					
T25					
T26	■				
T27					
T28					■
T29					
T30					
T31					
T32					
T33(9A)		■			■
T34(9B)		■			■
T35(9Γ)	■				
T36(9Δ)					
T37		■			■
T38				■	■
T39					
T40					
T41(7A)		■		■	■
T42(7B)				■	
T43(7Γ)				■	
T44(7Δ)				■	
T45		■			
T46		■		■	
T47					
T48		■			
T49(48A)		■			
T50		■		■	
T51				■	
T52					
T53				■	
T54				■	
T55					
T56(2A)		■			
T57		■			■
T58		■		■	
T59		■		■	■
T60		■		■	
T61(5A)		■		■	
T62(5B)				■	
T63		■			
T64(63A)		■			
T65		■			
T66(65A)					
T67(65B)					
T68				■	
T69					
T70					
T71					
T72					
T73					
T74				■	
T75					
T76		■			
T77					
T78					
T79		■			■
T80					
T81(80A)					

T82(80B)					
T83(80Γ)					
T84					
T85					
T86					
T87					
T88		■			
T89		■			
T90					
T91(90A)					
T92(90B)					
T93		■			
T94		■			
T95(94A)					
T96		■			
T97					
T98					
T99(98A)				■	
T100(98B)				■	
T101					
T102	■	■			■
T103(102A)					■
T104(102B)					■
T105					
T106		■			
T107		■			
T108					
T109(108A)				■	
T110	■	■			
T111					
T112					
T113		■			
T114					
T115		■			
T116		■			■
T117		■			
T118		■		■	
T119		■			
T120		■			■
T121		■			■
T122		■			

T123					■
T124		■			
T125					
T126		■			■
T127		■			
T128			■		
T129		■			■
T130					
T131		■		■	■
T132				■	■
T133				■	■
T134(19A)		■			
T135(19B)					■
T136(19Γ)					■
T137(19Δ)					
T138		■			
T139(138A)					
T140(138B)		■		■	
T141					
T142(141A)					
T143					
T144		■			
T145		■			
T146		■			■
T147		■			
T148			■		■
T149		■			■
T150				■	■
T151(150A)		■			■
T152(150B)					■
T153(150Γ)					■
T154		■			
T155(154A)		■			■
T156(154B)		■			
T157		■			
T158				■	
T159					
T160			■		
T161		■		■	
T162				■	
T163		■			■
T164					■
T165					■

Table 4. Schmidt hammer measurements in R-values

Tafoni	Backwall (MPa)	Floor (MPa)	Visor (MPa)	Ceiling (MPa)	Outer Roof (MPa)	Unweathered Rock (MPa)
T1	14					16
T2	13	14	9		11	15
T3	16	16				17
T4						17
T5						
T6		10			6	
T7	13			11	10	15
T8				13		17
T9	16	18		11		17
T10	10					12
T11						13
T12						14
T13						12
T14	9	11				12
T15						13
T16						10
T17						10
T18						10
T19	12			9		15
T20						11
T21						14
T22	14	14				16
T23						16
T24						15
T25						15
T26			17			
T27						15
T28						14
T29						13
T30						14
T31						11
T32						15
T33(9A)	16					17
T34(9B)	15					17
T35(9Γ)	15		11		9	16
T36(9Δ)						17
T37						16
T38						16
T39						16
T40						13
T41(7A)						15
T42(7B)	6					15
T43(7Γ)						15
T44(7Δ)						15
T45						14
T46						14
T47						14
T48	13					14
T49(48A)						14
T50						14
T51		11				15
T52						15
T53						12
T54						13
T55						11
T56(2A)	12					15
T57						14
T58						14
T59						10
T60						10
T61(5A)						
T62(5B)						
T63						12
T64(63A)						14
T65	11					14
T66(65A)						14
T67(65B)						14
T68	10					12
T69						12
T70						12
T71						13
T72						13
T73		12				16
T74		14				16
T75						16
T76						14
T77						14
T78						13
T79						10
T80	11					13
T81(80A)						13

T82(80B)						13
T83(80Γ)						13
T84						16
T85						16
T86						17
T87						17
T88						14
T89						14
T90	15					17
T91(90A)	15					17
T92(90B)	15					17
T93						12
T94	9	5				13
T95(94A)						13
T96	12					14
T97						14
T98						13
T99(98A)						13
T100(98B)						13
T101						17
T102						15
T103(102A)						15
T104(102B)						15
T105						11
T106						11
T107	11					13
T108	8					10
T109(108A)						10
T110	14		9	13	10	17
T111						14
T112						13
T113						12
T114						13
T115						13
T116	11					14
T117	4					14
T118						11
T119						12
T120						14
T121	14					17
T122						13

T123						13
T124						11
T125						13
T126		10				12
T127						9
T128						13
T129						17
T130						16
T131						16
T132						11
T133	7	9				12
T134(19A)	12	12				15
T135(19B)						15
T136(19Γ)						15
T137(19Δ)						15
T138						13
T139(138A)						13
T140(138B)						13
T141						11
T142(141A)						11
T143						13
T144						12
T145	13					16
T146						12
T147						12
T148						17
T149						17
T150	11					14
T151(150A)						14
T152(150B)						14
T153(150Γ)						14
T154						12
T155(154A)						12
T156(154B)						12
T157						16
T158						
T159		10				13
T160						16
T161						16
T162						14
T163		14				
T164						
T165						
Min	4	5	9	9	6	9
Max	16	18	17	13	11	17

[a]Faculty of Geology and Geoenvironment, National and Kapodistrian University of Athens, Panepistimiopolis, Zografou, 15784 Athens, Greece (evelpidou@geol.uoa.gr)
[*]Corresponding author.
[b]Faculty of Geology, University of Patras